

EUCREM Final Report

January 1998

Centre for Global Atmospheric Modelling, University of Reading, UK

M. Blackburn & E. Ioannidou

Summary

The five EUCREM cases have been simulated in a single column version of the UGAMP GCM, to evaluate the shallow and deep components of the Betts-Miller convective parametrization. The behaviour of other parametrizations in the single column model (SCM) is also highlighted by the simulations and sensitivity experiments.

Deep convection simulations with the Betts-Miller scheme are extremely successful in obtaining smooth evolution compared to the other EUCREM groups. Dependent on the convective adjustment timescale, grid scale saturation occurs in the presence of strong adiabatic forcing and a stratiform condensation-evaporation couplet is formed in the upper troposphere, effectively modelling aspects of a mesoscale anvil. The low-level parametrized downdraught acts to stabilise the sub-cloud layer and, through its interaction with the turbulence scheme, to increase the surface fluxes.

The shallow convection scheme, although not formulated to represent stratocumulus cloud, simulates the cumulus cases successfully. The main deficiencies are that convective cloud top cooling and moistening are not well constrained and the slope of the reference profile is not always optimal, deviating from the theoretical mixing line on which the scheme is based. Technical changes could improve these aspects. A closure for the convective adjustment timescale is required to represent the wide range of surface forcing and convective intensity in the EUCREM cases. The shallow convection scheme and present turbulence scheme do not interact well, since neither represents the effect of large eddies in the sub-cloud layer in the convective regime. A non-local turbulence closure would be more appropriate than the present local stability dependence in the convective boundary layer. Adjustment of the sub-cloud layer by the convection scheme would improve interaction of the parametrizations.

Noise and intermittency associated with the local turbulence closure scheme are evident in the strongly surface-forced cold-air outbreak. Unrealistic feedback between the turbulence and both convection and stratiform condensation via the stability profile contaminates the evolution, suggesting additional numerical advantages for non-local turbulence closure.

Not surprisingly the diagnostic cloud scheme performs poorly in many respects compared to newer prognostic schemes. The scaling of cloud fraction in terms of precipitation must be modified for non-tropical applications. Ideas are presented to make the scheme more physically consistent with the convective and stratiform processes in the SCM.

SCM Development

A single column version of UGAMP GCM version 2.1 has been used in EUCREM to evaluate and develop the Betts-Miller convective adjustment scheme (Betts & Miller 1993). The remaining parametrizations in the model are described in Slingo et al (1994) and consist of a Louis et al local, stability-dependent turbulence scheme, a condensation scheme to precipitate supersaturation, a diagnostic cloud scheme (Slingo 1987) and (where used) the radiation

scheme of Morcrette (1990). The turbulence, condensation and cloud parametrizations are based on and similar to those in the 1990 version of the ECMWF model, so can no longer be considered “state of the art” for operational models. Indeed several of the findings reported here highlight shortcomings of these parametrizations.

The SCM has been developed both scientifically and technically for EUCREM, resulting in a more flexible tool for parametrization evaluation and development.

Adiabatic forcing in the SCM has been extended to include prescribed divergence and thus interactive vertical advection, as required by EUCREM cases A and B. An option for prescribed surface fluxes has also been added, requiring modification of the implicit solution for the turbulent flux profile in the Louis et al scheme.

Cloud fraction and cloud water/ice content are important diagnostics for all the cases. The diagnostic cloud scheme computes these quantities from the convection scheme, relative humidity and other quantities, but it was previously called only at “full” radiation timesteps, typically 3 hourly. The cloud scheme is now called at every timestep in the SCM to provide continuous cloud diagnostics. These are used in the cloud-top cooling algorithm in case A.

Diagnostic routines have been added to write time series of SCM profiles and surface parameters using the DRS data structure used widely in the GCM community. This has allowed rapid viewing and additional diagnostic computation using a graphical workbench (VCS) supplied by PCMDI at Livermore. Formatted diagnostic output has also been added for the EUCREM intercomparisons.

Since the Betts-Miller scheme currently does not include momentum transports and the current study focuses on thermodynamic quantities, the SCM omits a momentum prognosis. Instead the wind profile is maintained at its initial state and turbulent momentum fluxes are neglected. This is equivalent to adding a momentum forcing to balance exactly the turbulent forcing at each timestep. While this will affect the turbulent heat and momentum fluxes in the sub-cloud layer, via the wind profile used in the local turbulence closure, the main results are not believed to be sensitive to this restriction.

The Betts-Miller convective adjustment scheme

The Betts-Miller convective adjustment scheme is described in detail in Betts and Miller (1993). The parametrization consists of separate deep precipitating and shallow non-precipitating schemes, the choice in any grid column depending initially on cloud-top height deduced from a parcel ascent. Each scheme computes a reference profile for temperature and specific humidity and the atmosphere is relaxed towards this on a prescribed timescale. For shallow convection the timescale has no theoretical dependence on horizontal resolution and the 4-hour timescale used in the UGAMP GCM is used for all the EUCREM cases. For deep convection the timescale should reduce with increasing resolution in a GCM, to counter the effect of stronger peak ascent rates. For resolutions of 100-150km, which is the CRM domain size for the deep convection cases, GCM experience suggests a timescale of 1 hour.

The shallow convection scheme is based on the concept of mixing the conserved saturation point properties between the sub-cloud layer and inversion top. For broken cumulus (i.e. a subsaturated grid-scale average) the conserved variables reduce to the potential temperature

and water vapour content (θ, q_v) but for stratocumulus the cloud water must be included. The scheme is currently formulated only for broken cumulus and has yet to be extended to stratocumulus. This is discussed further in case A below. Shallow convection does not adjust the sub-cloud layer, which is affected only by the dry turbulence scheme.

The deep convection scheme computes a neutral buoyancy profile, including virtual effects and liquid water loading up to the freezing level, and the column is adjusted towards it. The moisture reference profile is empirically based and consists of a subsaturation profile. The sub-cloud layer is adjusted towards an evaporatively driven downdraught profile, with its own timescale derived from an evaporation efficiency. If a deep cloud-top is diagnosed but the atmospheric column is too dry to precipitate, shallow convection is invoked instead (this is denoted a “swap point”).

Initial data, vertical and temporal resolution

Previous experience of the behaviour of the GCM parametrizations was gained at a standard 19-level vertical resolution, with approximately 100hPa spacing in the mid troposphere and 4 levels in the lowest kilometre. Initial SCM experiments used this resolution but the results were generally more sensitive to parametrization options than to resolution, so the results presented here and used for the intercomparisons use the 31-level resolution and spacing of the current operational ECMWF model. This has approximately 45hPa spacing in mid-troposphere and 5 levels in the lowest kilometre.

The initial data and (where required) adiabatic forcing data supplied by the CRM groups for each case have been interpolated to the standard 31-level resolution, by first integrating the piecewise linear profiles hydrostatically to obtain pressures and then interpolating the thermodynamic and momentum profiles to the model level pressures. Extrapolation above the “active” domain to the SCM top at 10hPa used data from radiosondes, if available, or the ECMWF reanalysis climatology for the relevant latitude and month.

Time discretisation was chosen as a compromise between typical GCM timestepping and a 5 minute sampling requested for some of the cases. Relatively minor sensitivity to timestep was found. The deep convection cases use a 15 minute timestep, the cold-air outbreak 10 minutes and the cumulus and stratocumulus cases 5 minutes. The SCM retains the leapfrog time-scheme of the GCM, rather than a simple forward scheme, leading to discrepancies between the time averages of the parametrization forcing computed directly and as a residual. This is most noticeable in the cold-air outbreak, where the evolution is more intermittent.

Case A: North Atlantic Stratocumulus

The Betts-Miller shallow convection scheme is currently formulated in terms of mixing the mean profiles of potential temperature and water vapour (θ, q_v), which are conserved variables for broken cumulus only. To simulate stratocumulus successfully, where the mean profile is supersaturated, transformation to liquid water potential temperature and total water content (θ_l, q_t) would be required. The SCM does not predict a cloud water variable and the condensation and diagnostic cloud schemes would also require modification to maintain grid-averaged supersaturation during a simulation.

The prescribed initial data includes a stratocumulus cloud sheet with adiabatic water content.

This cloud water has been removed to leave the cloud layer just at saturation, and cloud water is instead diagnosed from the cloud scheme at each timestep and used in the prescribed cloud-top longwave cooling algorithm. If supersaturation occurred during the integration it would be immediately precipitated, but the large scale descent is sufficient to prevent this and there is no drizzle. This experimental setup differs from the formal case specification, but is how a GCM of this type would handle stratocumulus situations, so it is nevertheless instructive. For this reason the experiments described here have not been included in the formal intercomparison, though the CRM and other SCM results have been used in the diagnostic analysis.

Despite grid scale saturation, the cloud scheme initially diagnoses only ~20% cloud cover from its empirical inversion criterion and ~25% from a pseudo condensation rate in the convection scheme. The cloud scheme assumes 1% supersaturation, so the resulting cloud water path is only 3.4% of that implied by the prescribed adiabatic in-cloud profile. The resulting longwave cooling is 82% of that prescribed but is spread over the two in-cloud levels rather than being entirely in the top layer. Clearly the cloud-scheme is not optimised for this case and gives both the low cloud fraction and weak radiative effect expected of this generation of GCM for stratocumulus conditions.

Fig.1 shows the evolution of radiative cooling and turbulence-plus-cloud heating and moistening (Q1 and Q2) for a control integration using the default Betts-Miller parameters. Convection is maintained for 13 hours, ceasing shortly after the cloud radiative cooling weakens. The origin of this breakdown is in the moistening profile, Q2. This is noisy from the beginning, due to poor overlap of the turbulent and convective moistening, and there is even drying initially at the inversion top (see below). The weak moistening of the cloud layer cannot balance the large scale descent drying, causing the relative humidity at the inversion base to reduce. This eventually reduces the diagnosed cloud fraction via a humidity criterion in the cloud scheme, and this in turn reduces the diagnosed cloud water and radiative cooling. The adiabatic warming then dominates, stabilising the cloud layer and causing convection to cease. Thus the maintenance of (strato)cumulus relies on cloud-top radiative cooling and the cloud break-up process is simulated realistically. The main sensitivities of the evolution are to the convective forcing, which depends on parameters in the convection scheme, and to the descent rate, which is relatively uncertain for this case and tuned to give observed inversion height in the CRM simulations (it differs in the GCSS version of this case by a factor of 3).

The shallow convection scheme mixes through the cloud layer and into the inversion as required, but an analysis in terms of mixing of the conserved variables, using the profile of saturation point quantities which is the basis of the scheme, reveals some shortcomings. Using the default mixing parameters for the scheme, the inversion top is initially moved almost perpendicular rather than parallel to the mixing line between sub-cloud and inversion-top air (Fig.2). This involves both cooling and drying of air at the inversion top, which is unphysical since the mixing process must theoretically cool and moisten this level by evaporation of cloud water. Clearly the current technical formulation of the scheme does not constrain it to mix the conserved variables as required. The reason in this case is that the reference profile in Fig.2 has a slope in conserved variable space differing from the theoretical mixing line, due to an empirical slope parameter which is inappropriate in this case. An interactive determination of the slope parameter is required to ensure that the ratio of convective tendencies (Q1/Q2) is constrained always to be parallel to the mixing line.

In earlier experiments the turbulence acted strongly only at the surface and in the inversion,

due to an erroneous interpolation of the initial data. This revealed extreme sensitivity of the local turbulence closure to small changes in Richardson number. In the simulations reported here, turbulence acts smoothly through the sub-cloud layer.

Case B: North Sea Cumulus

In common with the other EUCREM groups, spin-up problems were encountered using the original specification of the initial data. The parametrizations removed kinks in the piecewise linear moisture profile in the first few hours. Additionally in the UGAMP SCM, the local turbulence closure created noisy turbulent flux profiles during the spin-up, highlighting the sensitivity of a local scheme to discontinuities in the stability profile.

The revised initial data, with a more continuous moisture gradient, leads to smoother evolution and reduced spin-up. However there is evidence of a systematically different spin-up in this and the other SCMs to that in the CRMs. In the SCM, parametrized turbulence begins only in the surface layer, since the initial sub-cloud layer is slightly statically stable, but parametrized convection begins immediately, since small negative CAPE below cloud base does not inhibit convection (Fig. 3). Mixing therefore occurs in the cloud layer and inversion immediately, while small scale turbulence takes 1-2 hours to fill the sub-cloud layer. In contrast, the CRMs take 2 hours or more to develop mixing from the surface through to the inversion. By 3-4 hours, the period of the intercomparison diagnostics, the CRMs and SCM are therefore acting on different thermodynamic profiles, though the importance of this is uncertain. Future intercomparisons could achieve greater consistency by spinning up turbulence and convection for several hours while relaxing the mean state to the observed initial profile, allowing the free-running evolution to begin from a common initial state in which clouds and turbulence are already in quasi-equilibrium. This procedure would also allow closer comparison with the observations.

The evolution of the “control” simulation is shown in Fig.3 over an extended period of 12 hours. The initial convective forcing evolves into a profile which is robust to changes in the Betts-Miller scheme parameters, in which mixing of cloudy air into the inversion counteracts, but is weaker than, both the descent warming and drying. There is intermittency in the cloud base level, possibly because the observed cloud base and initial lifting condensation level are very close to a model level. The subcloud layer warms and moistens from the prescribed surface fluxes, its profile evolving consistently in all the models to become slightly statically unstable and with increased moisture lapse than initially (not shown). The Q2 moistening profile in the UGAMP SCM remains noisy because of poor overlap between the parametrized turbulence and convection, as in case A. A crude attempt to allow convection to adjust below cloud base gives an improved simulation, with a smoother Q2 profile and reduced intermittency of cloud base level. As a result, a modified version of the scheme which adjusts the entire sub-cloud layer will be tested.

Parametric analysis, using the profile of conserved saturation point properties, shows the convective tendencies at the inversion top to be poorly constrained, as in Case A (Fig.4). In this case the sensitivity is to a parameter controlling the degree of mixing in the inversion. The scheme’s default parameter ($B_{inv}=2.5$) leads to insufficient mixing initially because, as is clear in Fig. 4, the reference profile is not significantly compressed along the mixing line relative to the initial environmental profile. As a result the inversion forcing is weak and the corrections required for conservation have an undue influence, producing a Q1/Q2 ratio far

from that of the theoretical mixing line slope. Stronger inversion mixing (e.g. $B_{inv}=2$ in Fig.4) results in a more compressed reference profile and a Q1/Q2 ratio nearer its theoretical value. As mentioned previously, the initial convective forcing evolves into a more robust profile as the mean state adjusts, but the initial sensitivity suggests a different approach to defining the inversion mixing, possibly using a criterion for cloud-top entrainment instability. This could also be used to distinguish between cumulus and stratocumulus cloud fractions. The CRM data have yet to be used to estimate or constrain the inversion mixing.

The cloud scheme diagnoses between 10% and 40% cloud cover, the fraction being sensitive to the number of model levels in cloud. The upper limit is an overestimate similar to that in the other SCMs in the intercomparison: if interactive radiation was included this would lead to incorrect cloud radiative forcing.

It is the Betts-Miller shallow scheme which performs the adjustment in this case, despite the cloud top height being classed as deep over sea by the parametrization. Deep convection is attempted first, but the convecting layer contains insufficient humidity to sustain precipitation and the scheme “swaps” to shallow convection instead. The scheme’s switching logic is discussed further in case C, where it is more of an issue.

Case C: Arctic Cold-air Outbreak

Control and sensitivity simulations for case C follow the case specification of placing the initial ice-edge atmospheric profile over a fixed SST of 1.5degC and integrating for a period of at least 20 hours. Separate roughness lengths for momentum and heat were specified but the turbulence scheme allows only a single value for all variables. However interactive surface fluxes with roughness length based on the Charnock relation give almost exactly the prescribed roughness length for momentum throughout the integration period, so interactive fluxes have been used in all the simulations. The intercomparison shows that the resulting surface fluxes are comparable with those in the other models and with values derived from the observations. Most of the simulations omit radiation, but experiments with interactive radiation are also described below.

There is discrepancy in the initial moisture content between the models, since a relative humidity profile was prescribed and different saturation criteria have been used to convert to specific humidity. While most groups use water saturation at all temperatures, the UGAMP SCM uses ice saturation below freezing point and precipitates all moisture in excess of this. ECMWF use a mixed phase formulation between zero and -23degC. Low level specific humidity increases by a factor of five through the simulation, so details of the initial profile are relatively unimportant.

The SCM successfully simulates a deepening cloudy boundary layer which warms and moistens approximately as observed, due to the strong surface forcing. Turbulence and shallow non-precipitating convection are invoked from the start, with precipitating convection occurring once the cloud top reaches approximately 800hPa, after 11 hours. After this the convection alternates between the two types, though with a fixed cloud top, as the (implicit) humidity criterion of the deep scheme is not maintained. In contrast to the other shallow convection cases, turbulence extends into the cloud layer, giving a more continuous upward moisture flux, because the in-cloud stability (approximating a moist adiabat) has very low static stability here, due to the low absolute moisture content. This contrasts with the mid-

latitude and tropical cases, where a marked increase in static stability and Richardson number at cloud base effectively restricts turbulence to the sub-cloud layer in the SCM.

For the default shallow convective adjustment timescale of 4 hours, which is based largely on trade wind cumulus studies, the convective fluxes are much weaker than the turbulent fluxes. A timescale of 1 hour is more appropriate for this strongly surface forced case and clearly an interactive closure for timescale is required, based on the surface sensible heat flux directly or on a CAPE adjustment timescale, if the scheme is to simulate the range of convective intensity in the EUCREM cases.

Two robust features of the evolution reveal important deficiencies in the SCM parametrizations.

First, the boundary layer quickly becomes saturated throughout its depth and remains saturated for the entire simulation (Fig.5), moister than all other simulations in the intercomparison. The main reason for this is the non-precipitating nature of the shallow convection scheme, which transports moisture upwards but is unable to reduce the integrated moisture content. Until cloud-top reaches the threshold for deep convection, latent heating can occur only in the stratiform precipitation scheme and this requires grid-scale saturation. In addition, falling precipitation evaporates in each level below cloud until saturation is reached, so a saturated column between the initial condensation level and the surface is created before stratiform precipitation reaches the surface. This has implications for both the column moisture and heat budgets. Not only is the amount of water vapour stored in the column maximised, but the saturated surface layer inhibits further evaporation. Both effects reduce the column latent heating and temperature increase so that, later in the simulation, the SCM is the coldest of the intercomparison. This effect is likely to be larger at higher temperatures, where a given relative humidity is associated with a higher absolute humidity content, so the GCM is likely systematically to underestimate warming in cold-air outbreaks in the oceanic storm-tracks. Sensitivity experiments for this case, in which evaporation of falling precipitation is inhibited, lead to stronger heating and a deepening sub-saturated sub-cloud layer, in better agreement with the other models and observations. However, allowing shallow convection to precipitate would be a more physically based solution to this problem.

Second, the evolution is very noisy with intense 4-timestep variability in parametrized heating and moistening rates (Fig.6). Although details of the noise are sensitive to the convective timescale, a simulation without convection reveals that the problem is caused by interaction between turbulence and stratiform condensation, via the local Richardson number turbulent closure. The intense surface forcing initially acts to increase low level relative humidity rapidly (for the latent/sensible flux ratio near 1/3 and low saturation humidity at the cold temperature), and the resulting latent heating changes the Richardson number profile, affecting turbulent mixing at the subsequent timestep. Evaporation beneath condensation in the boundary layer strengthens the feedback, and removal of stratiform evaporation localises intermittency to the upper part of the boundary layer in the later stages of the simulation. The intermittency period is predominantly 4-timesteps because of the leapfrog time differencing with time-lagged input to the parametrizations. Maintenance of grid-scale subsaturation by a precipitating shallow convection scheme would undoubtedly reduce the intermittency but a non local turbulence closure in convective situations would remove the strong local feedback which is the basic cause of the intermittency.

A lack of physical integration of the diagnostic cloud scheme with the remaining parametrizations is evident, since fractional cloud (of only a few percent) is diagnosed, despite grid-scale saturation. First, to avoid diagnosing low cloud at all ocean points in a GCM, no layer cloud is allowed in the lowest ~ 2 km from the relative humidity criterion, so layer cloud is diagnosed only when the moist boundary layer reaches roughly 800hPa. Second, the extremely small convective cloud fraction and water content are due to their empirical dependence on precipitation or condensation rate being based only on tropical data (Slingo 1987): the low absolute humidity in this case leads to small condensation rates. A crude rescaling of condensation by the ratio of the actual saturation humidity and a typical tropical value immediately gives cloud fraction near 50%, close to observed values, with correspondingly larger cloud water content. This has a large impact if interactive radiation is included in the simulations, increasing in-cloud radiative cooling from typically 0.7K/day to typically 2.5K/day.

This modification of the cloud scheme can be seen as a first step in making it more physically based, taking ideas from modern prognostic schemes but without including prognostic cloud variables in the model. The condensation rate is currently converted to convective cloud fraction using an empirical relation, and a simple cloud model (1% supersaturation) then gives cloud water content. Instead the condensation rate should be viewed as creating supersaturation and cloud water, with the cloud model then giving cloud fraction, dependent on the local saturation specific humidity. Additional information is then required, equivalent to a timescale over which condensation acts, to obtain cloud water content. In a prognostic scheme storage and accumulation across timesteps provide this scaling in a physically consistent way, plus a memory which cannot be built into a diagnostic scheme.

The deep convection cases

Both the experimental design and behaviour of the Betts-Miller convection scheme are very similar for the two deep convection cases. Both cases have been simulated as prescribed, using adiabatic forcing of temperature and moisture computed from the CNRM CRM. The CRM has been integrated with open boundary conditions, allowing mesoscale ascent to develop in the domain as a response to the convective forcing. In order to compare the SCM and CRM simulations, it is only consistent to run the SCM with parametrized and forcing processes (e.g. surface fluxes, radiation) included or excluded exactly as in the CRM integration. Nevertheless, sensitivity tests have been made varying these processes, in order to understand the behaviour of the control simulations.

The simulations enable analysis of the parametrized convective response to mesoscale forcing, but there is a wider question of how to represent such a situation in a GCM. At high resolutions typical of current deterministic forecasting or regional models, the mesoscale flow would be at least partially resolved and would arise as a response to localised convection, allowing feedback between convection and mesoscale dynamics. This is an interactive analogue of the SCM experiments here. However at resolutions typical of GCM climate modelling such interaction cannot be modelled explicitly and the mesoscale forcing would need to be parametrized within the convection and cloud schemes. It is not clear how this is to be done and the experiments described here do not address this question.

The timescale of the Betts-Miller deep convective adjustment is intended to vary with horizontal resolution, as described previously. Experience at ECMWF and in UGAMP

suggests that a 1 hour timescale may be appropriate for a GCM resolution of 100-150km, which is the range of CRM domain size in the deep cases. Experiments for case E show the SCM sensitivity to timescale. The convective gustiness enhancement of the surface fluxes, included in the GCM and discussed in Slingo et al (1994), is not included in the SCM.

Case D: Central European Thunderstorms

Case D has been successfully simulated for the prescribed 6 hour period using a 15 minute timestep, starting from the lifted Payern sounding supplied by DLR and including the CRM adiabatic forcing. The CRM simulation excluded radiation but included interactive surface fluxes, using a roughness length typical of the region, following problems using the prescribed constant fluxes throughout the CRM domain. The SCM simulations have been performed both with constant fluxes, using either 100% or 60% of the prescribed 530W/m² latent and 150W/m² sensible flux, and also with interactive fluxes, using a roughness length and surface temperature identical to those in the CNRM CRM simulation.

Fig.7 shows that the evolution of surface precipitation in the SCM is smooth and that there is little sensitivity to the surface forcing, highlighting the predominance of the adiabatic forcing in determining convective response. With mid-level adiabatic cooling and moistening in excess of 100K/day and 40g/kg/day respectively after 6 hours, the convection must almost cancel the forcing if the temperature and moisture profiles are not to change by unrealistically large amounts. The timeseries of precipitation, increasing to reach 160-170mm/day after 6 hours, reflects this balance. For comparison, if the total energy input from the surface heated a 500hPa layer (by both sensible and latent heating), the 680W/m² of the 100% prescribed flux case would convert to roughly 11K/day, less than 10% of the peak adiabatic forcing. Radiation, if included, would be a yet weaker component of the budget.

With interactive surface fluxes the land surface cools rapidly, due to strong initial turbulent heat loss and a lack of radiative forcing, and the surface layer cools by an unrealistic 5K within 90 minutes. This causes the surface fluxes to asymptote to values significantly smaller than those prescribed. Despite this cooling, the convection and precipitation in Fig.7 remain almost as intense as with prescribed fluxes.

Compared with the other SCMs, the precipitation evolution is consistently smooth and without noticeable spin-up. This is true also of the convective heating and moistening profiles, shown in Fig.8 for the 100% prescribed surface flux case, together with the stratiform heating and moistening and the temperature and moisture evolution.

Deep convection is invoked from the start and the initial evolution is dominated by adjustment towards the BM deep reference profile on the 1 hour adjustment timescale. This reveals a limitation of the convection scheme, in that it will adjust any deep unstable profile to the reference structure, removing short length-scale vertical structures in the environmental profile. After the initial adjustment, the convection intensifies with the adiabatic forcing, approximately balancing it. However the forcing soon saturates the upper troposphere and the stratiform condensation scheme produces a condensation-evaporation couplet of increasing strength, which progressively extends to lower levels. This feature is effectively a mesoscale anvil which occupies the entire horizontal extent of the grid square. Its time of onset and strength are dependent mainly on the convective adjustment timescale, with onset after 4 hours for the default 1 hour timescale. A shorter timescale allows the convection to balance the

forcing more closely, so that relative humidity increases more slowly, the opposite being true for a longer timescale. The saturated layer reaches the surface in the last hour of the simulation, leading to the onset of (weak) stratiform surface precipitation.

In contrast to the shallow convection cases, turbulence and convection appear to interact successfully with little intermittency. This is almost certainly due to the near neutral initial profile at low levels and the convective downdraught parametrization, which adjusts the sub-cloud-layer toward a sub-saturated profile with well defined stability. However the downdraught is not entirely realistic, since the initial adjustment creates a sub-cloud layer (potentially) warmer than the cloud above. This appears to be due to a technical restriction on downdraught depth, yet to be removed, which results in the cloud base implied by the downdraught depth being significantly lower than that in the initial sounding. In the last hour the intensifying downdraught strongly stabilises the sub-cloud layer and intermittency occurs in the turbulent moisture flux profile when using prescribed surface fluxes, as the fluxes strongly heat and moisten a shallow surface layer. This suggests that, for numerical reasons, any non-local turbulence closure should be used not only in conditions of static instability, but also in the presence of deep convective downdraughts. In reality the downdraught occupies only a fraction of the grid box, coexisting with large convective eddies in updraught regions.

Despite diagnosing an increasing cloud fraction with time, reaching 80% in 2 hours and total cover after 3 hours, the vertical profiles of cloud fraction and water content are very crude and not linked directly to the convective and stratiform processes occurring at each timestep. Convective cloud fraction has a maximum of 20% in depth, with 80% at the first level above cloud-base (representing ubiquitous shallow clouds) and a similar anvil fraction at the top in-cloud level. Despite grid-average saturation and stratiform precipitation at mid-levels later in the simulations, the cloud scheme does not diagnose mid-level stratiform cloud, because the relative humidity criterion is adjusted for assumed supersaturation in the convective cloud. Clearly the diagnostic cloud should be more consistent with both the convective and stratiform processes occurring in the column.

Case E: Tropical Pacific Squall Line

The SCM simulations of the Pacific squall line exhibit the same basic characteristics as the continental European thunderstorms case, since the experimental set up is very similar. The main differences from the continental case are somewhat weaker adiabatic forcing, resulting in a larger influence of surface fluxes, and a lower cloud base, resulting in a more realistically modelled low-level downdraught.

The SCM has been integrated for 7 hours from the prescribed initial sounding, including the adiabatic forcing from the “SURFRADICE” experiment of the CNRM CRM. The SCM control integration similarly includes interactive surface fluxes and radiation and the convective adjustment timescale is 1 hour in the control simulation.

The convective and stratiform precipitation are shown in Fig.9 for adjustment timescales of 1 hour and 2 hours. The evolution is again smooth but in this case there is a marked spin-up in the first hour, as the initially moist sounding is dried towards the subsaturation profile of the convective reference state. The reference parameters are defined globally, rather than being computed interactively, dependent on ambient conditions and convective regime. While this may be valid for the temperature reference profile, which approximates neutral buoyancy, it is

more questionable for moisture. This also has implications for radiative transfer. After the initial adjustment, the precipitation increases smoothly in response to the increasing adiabatic forcing, with more moistening and less precipitation if a longer adjustment timescale is used. This affects the timing of grid-scale saturation and onset of stratiform processes, shown also in Fig.10, reflecting the ability of convection of a given intensity to prevent saturation. After 7 hours the total surface precipitation rate is almost independent of convective timescale (because the column has become saturated in depth) but weaker convection requires a stronger stratiform component.

Omission of radiation and/or interactive surface fluxes in the SCM is inconsistent with the adiabatic forcing data from the CRM, in which these processes were included, but does reveal the role of the parametrized low-level convective downdraught. If surface fluxes are omitted, deep convection ceases after 3 hours and becomes intermittent, despite increasing adiabatic forcing. The sub-cloud layer initially cools more quickly than before, removing the deep conditional instability, because the cooling effect of the low-level downdraught is no longer balanced by turbulence. The downdraught plays a dual role of inhibiting parcel ascent but increasing the surface fluxes to maintain instability. This is confirmed by reducing the downdraught efficiency from 15% to 5%, in which case the surface fluxes are reduced by roughly 30% by the end of the simulation.

If radiation is omitted instead, deep convection remains continuous, with almost identical evolution to the control simulation, demonstrating the strength of the adiabatic forcing. The largest effect of radiation is near cloud top, where strong radiative cooling above cloud and warming in cloud maintains a higher cloud top later in the simulation. However the convective heating profile is noisy and cloud top fluctuates, both being worse with radiative feedback. The noisy structure is known to be sensitive to the formulation of the energy correction in the deep convection scheme and requires further investigation. The problem is compounded by the use of intermittent “full radiation” timesteps in the UGAMP (and ECMWF) models, for computational efficiency. The SCM cloud diagnostics are hourly averaged and input to the radiation for the next hour, allowing the cloud thermodynamic and radiative forcings to become dissociated, both in time and height. This is evident in Fig. 10c,f.

As in case D, the diagnosed cloud fraction and cloud water content, used for the cloud radiative forcing, have an unrealistic vertical profile which is closely related only to the convective processes at each timestep. Complete cloud cover is diagnosed near convective cloud top throughout the simulations, representing a shallow anvil there, although stratiform condensation develops later and is not associated with a separate diagnosed cloud structure.

Discussion and Conclusions

EUCREM has provided a valuable context in which to evaluate the Betts-Miller convective adjustment scheme in the UGAMP SCM, providing a wide range of both convective regime and models with which to compare. The two years of this initial phase of EUCREM have allowed detailed evaluation and analysis of the current convective and associated parametrizations in the SCM and the main deficiencies found are reported here. The intention is not criticism of the parametrizations: rather it is now possible to focus on the improvements most likely to improve their realism and accuracy.

The Betts-Miller deep, precipitating convection scheme is extremely successful in giving a

smooth evolution of physical processes in both the continental and maritime cases studied. The scheme responds to the intense mesoscale forcing by moistening until stratiform processes occur, initially in the upper troposphere, representing a mesoscale anvil couplet of condensation and evaporation. The parametrized low-level downdraught plays an important role in cooling the sub-cloud layer and enhancing (interactive) surface fluxes, though a generalisation of downdraught depth is still required, particularly for continental convection.

For the Betts-Miller shallow convection scheme, attention has focused on the degree to which convection is constrained simply to mix sub-cloud and inversion-top air, using the saturation point analysis on which the scheme is based. Extension of the scheme to super-saturated conditions is necessary for a more realistic simulation of stratocumulus, but the diagnostic cloud and stratiform condensation schemes would require modification too. It is not yet clear whether significant improvement in cloud fraction and radiative impact can be attained within this framework, or whether a prognostic cloud scheme is required.

Interaction between shallow convection and turbulence parametrizations in the SCM has been shown to be deficient because convective (or “large”) eddies in the sub-cloud layer are not represented by either scheme. A non-local turbulence scheme for convective regimes is likely to improve this and to reduce intermittency associated with the present local turbulent closure.

The cold air outbreak case has more general implications for convective closure. It reveals that distinction between precipitating and non-precipitating convection based on cloud-top height alone is insufficient and that convective intensity should be related to the strength of the surface forcing and turbulence. Without this, the SCM can represent only stratiform precipitation in such cases, with excessive storage of moisture and consequent implications for column budgets and the rate of warming of cold air in the oceanic storm-tracks.

The diagnostic cloud scheme of the SCM is being superseded in operational models by prognostic schemes which integrate the cloud parametrizations in a more physically consistent manner. However, deficiencies in the SCM simulations have suggested that the diagnostic scheme could be more physically based, with condensation producing cloud water and a simple cloud model then giving cloud fraction, rather than the current reverse of this logic.

References

Betts, A. K. and M. J. Miller 1993 The Betts-Miller scheme. Chapter in *The representation of cumulus convection in numerical models of the atmosphere*. Eds. K. A. Emanuel and D. J. Raymond. American Meteorological Society.

Morcrette, J-J. 1990 Impact of changes to the radiation transfer parametrizations plus cloud optical properties in the ECMWF model. *Mon. Wea. Rev.*, **118**, 847-873.

Slingo, J. M. 1987 The development and verification of a cloud prediction scheme for the ECMWF model. *Q. J. R. Meteorol. Soc.*, **113**, 899-927.

Slingo, J. M., M. Blackburn, A. K. Betts, R. Brugge, K. D. Hodges, B. J. Hoskins, M. J. Miller, L. Steenman-Clark & J. Thurn. 1994 Mean climate and transience in the tropics of the UGAMP GCM. Part I: Sensitivity to convective parametrization. *Q. J. R. Meteorol. Soc.*, **120**, 881-922.

Figure Captions

Fig. 1. Case A control simulation, showing evolution of a) cloud and turbulent heating (Q_1) in K/day, b) cloud and turbulent moistening (Q_2) in g/kg/day and c) radiative heating in K/day. Radiative cooling extends over the entire cloud layer and its weakening after 12 hours is the precursor to the cessation of convection. The contour interval is approximately logarithmic.

Fig. 2. Conserved variable plot for Case A, showing the saturation point profile for the (modified) initial state. Also shown is the initial reference profile for the Betts-Miller scheme, which departs significantly from the theoretical mixing line between the surface layer and inversion top. Light arrows joining the initial profile to the reference profile depict the initial convective forcing, which is far from parallel to the mixing line.

Fig. 3. Evolution of parametrized heating (left, in K/day) and moistening (right, in g/kg/day) for the control simulation of Case B. Top panels show convective forcing and bottom panels turbulent forcing. The contour interval is approximately logarithmic.

Fig. 4. Conserved variable plot for Case B, showing the saturation point profile for the initial state. Also shown is the initial reference profile for the Betts-Miller scheme, for a range of the inversion mixing parameter (the control simulation uses a value of 2.5). The reference profile differs from the mixing line between the sub-cloud layer and inversion top. Light arrows joining the initial profile to one of the reference profiles depict the initial convective forcing, which also differs significantly from that predicted by the mixing theory.

Fig. 5. Evolution of the deepening boundary layer for the control simulation of Case C. a) Potential temperature, b) Specific humidity, c) relative humidity.

Fig. 6. Evolution of parametrized heating (left, in K/day) and moistening (right, in g/kg/day) for the control simulation of Case C, showing intermittency associated with the local turbulence closure interacting with stratiform condensation. Top panels show total parametrized forcing, middle panels show turbulence forcing and bottom panels show stratiform condensation forcing. Shading intervals are approximately logarithmic.

Fig. 7. Case D. Evolution of surface precipitation rate in mm/day, for interactive surface fluxes (solid), 100% prescribed fluxes (dotted) and 60% prescribed fluxes (dashed).

Fig. 8. Case D simulation with a convective adjustment timescale of 1 hour. Heating (left) and moistening (right), due to convection (top) and stratiform condensation (middle). Temperature and moisture evolution as departures from the initial state (bottom).

Fig. 9. Case E. Evolution of surface precipitation rate in mm/day, for a convective timescale of 1 hour (solid) and 2 hours (dashed).

Fig. 10. Case E simulations with a convective adjustment timescale of 1 hour (left) and 2 hours (right). Heating rates in K/day for deep convection (top), stratiform condensation (middle) and all parametrizations (bottom).

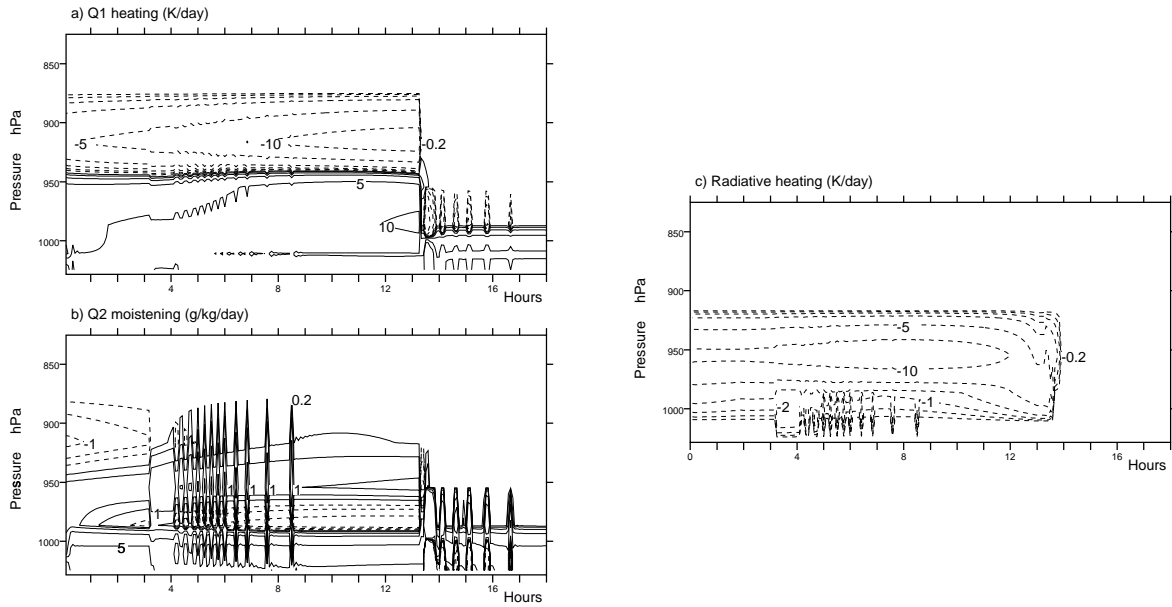


Fig. 1. Case A control simulation, showing evolution of a) cloud and turbulent heating ($Q1$) in K/day, b) cloud and turbulent moistening ($Q2$) in g/kg/day and c) radiative heating in K/day. Radiative cooling extends over the entire cloud layer and its weakening after 12 hours is the precursor to the cessation of convection. The contour interval is approximately logarithmic.

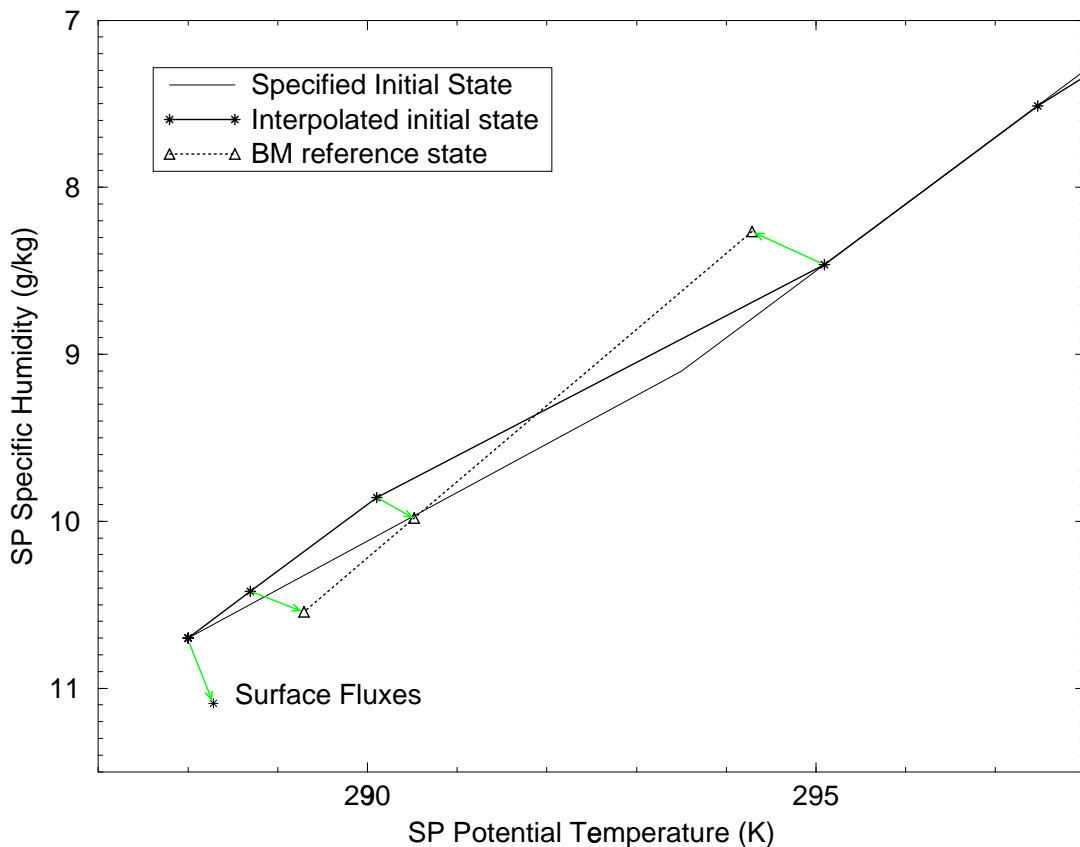


Fig. 2. Conserved variable plot for Case A, showing the saturation point profile for the (modified) initial state. Also shown is the initial reference profile for the Betts-Miller scheme, which departs significantly from the theoretical mixing line between the surface layer and inversion top. Light arrows joining the initial profile to the reference profile depict the initial convective forcing, which is far from parallel to the mixing line.

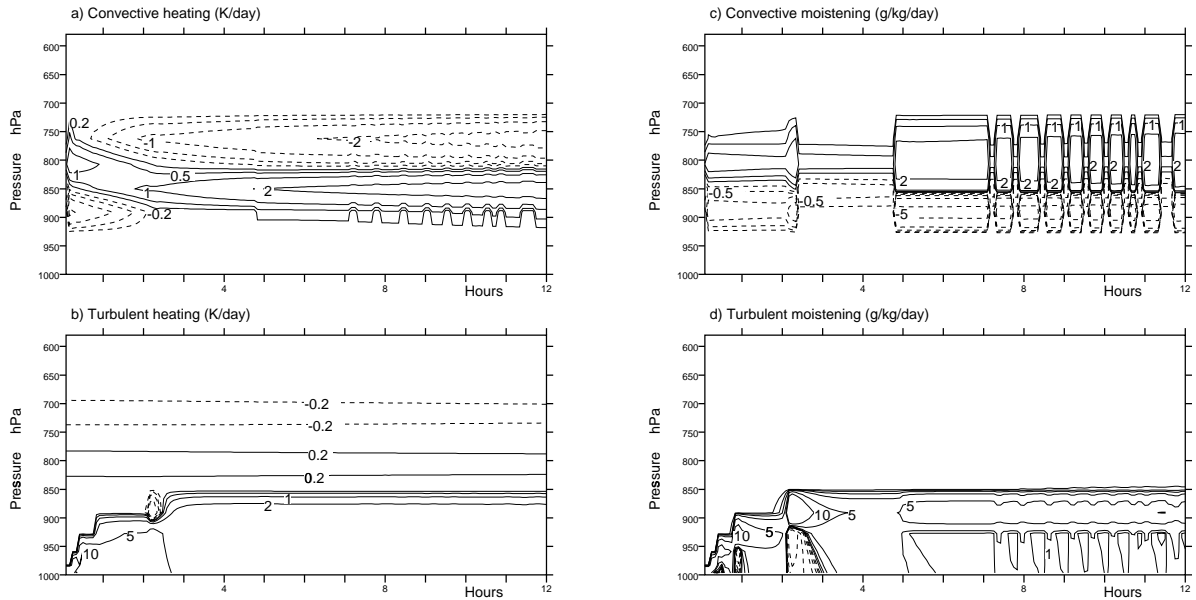


Fig. 3. Evolution of parametrized heating (left, in K/day) and moistening (right, in g/kg/day) for the control simulation of Case B. Top panels show convective forcing and bottom panels turbulent forcing. The contour interval is approximately logarithmic.

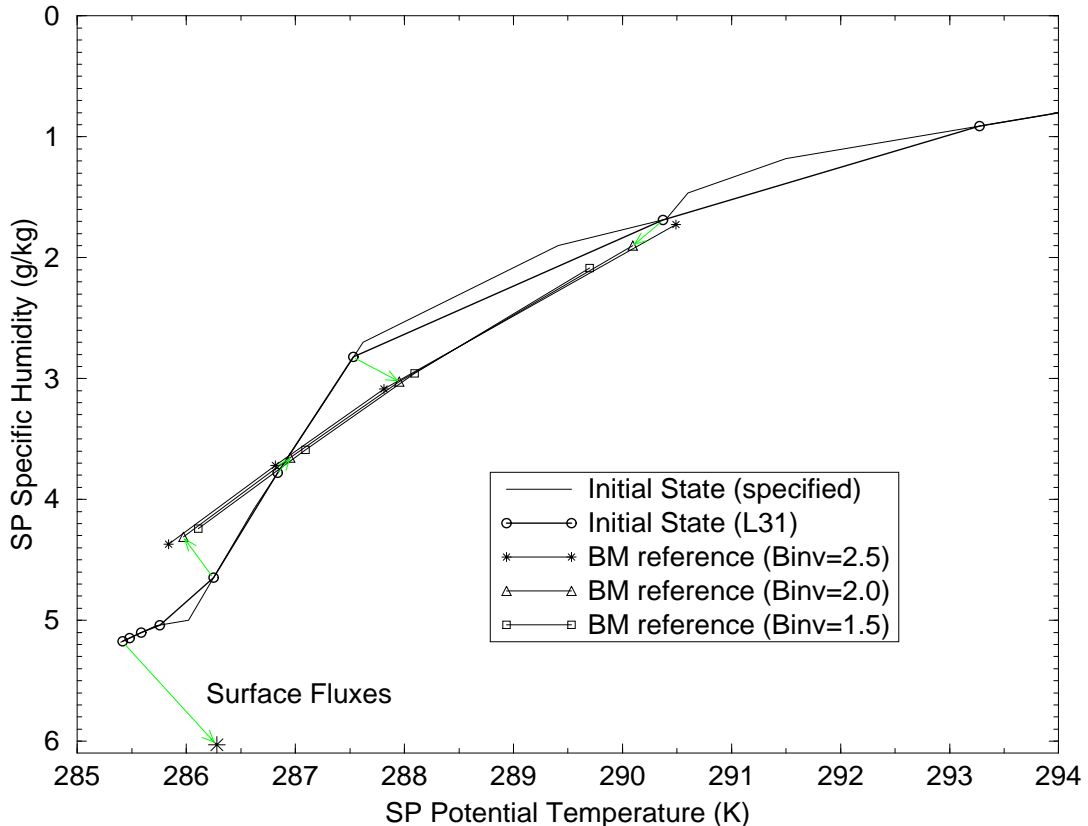


Fig. 4. Conserved variable plot for Case B, showing the saturation point profile for the initial state. Also shown is the initial reference profile for the Betts-Miller scheme, for a range of the inversion mixing parameter (the control simulation uses a value of 2.5). The reference profile differs from the mixing line between the sub-cloud layer and inversion top. Light arrows joining the initial profile to one of the reference profiles depict the initial convective forcing, which also differs significantly from that predicted by the mixing theory.

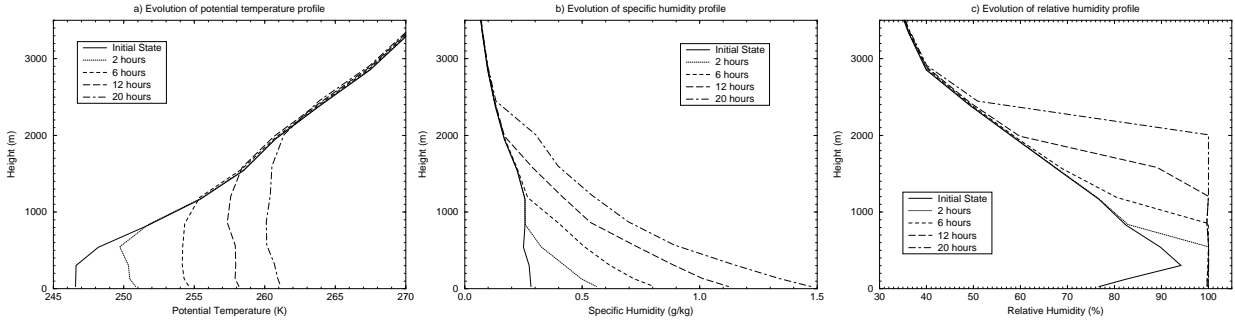


Fig. 5. Evolution of the deepening boundary layer for the control simulation of Case C. a) Potential temperature, b) Specific humidity, c) relative humidity.

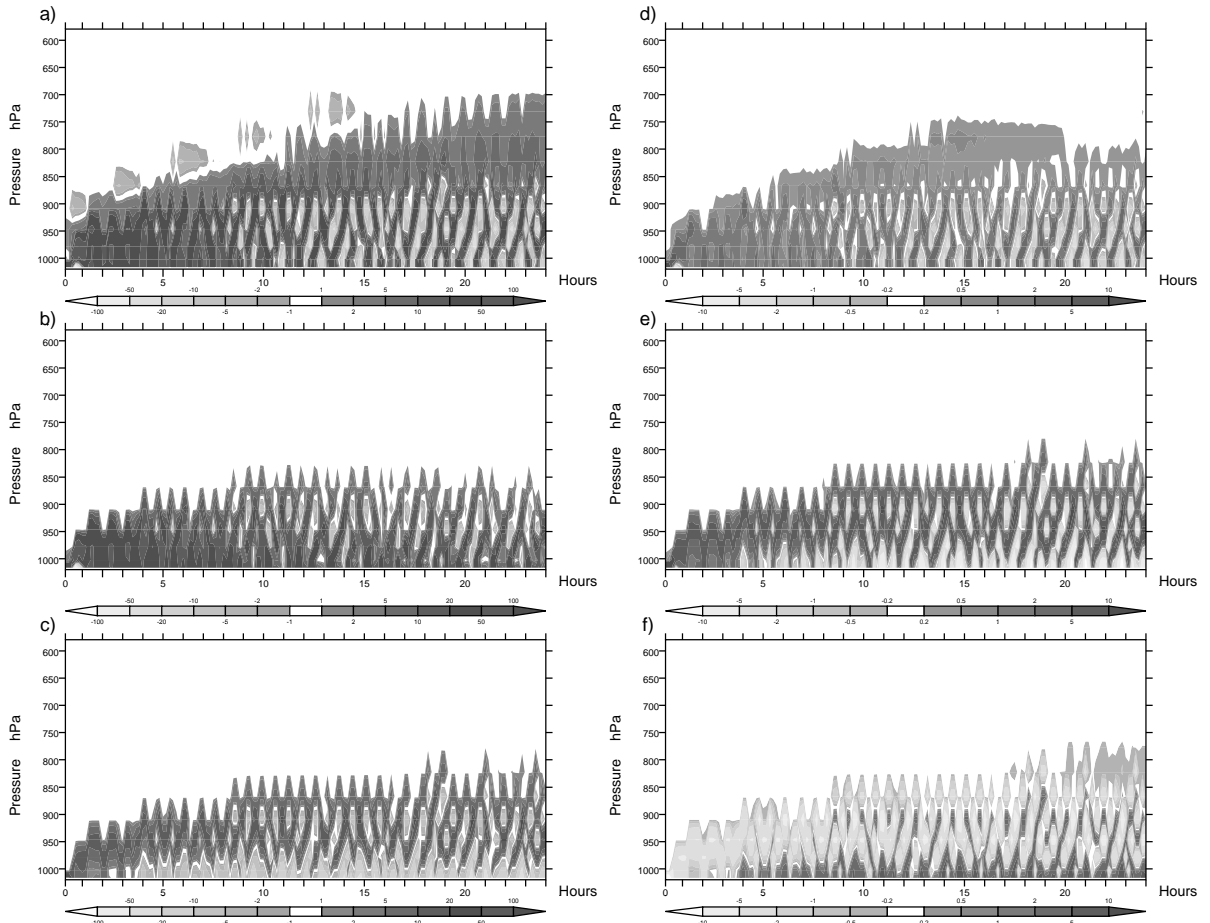


Fig. 6. Evolution of parametrized heating (left, in K/day) and moistening (right, in g/kg/day) for the control simulation of Case C, showing intermittency associated with the local turbulence closure interacting with stratiform condensation. Top panels show total parametrized forcing, middle panels show turbulence forcing and bottom panels show stratiform condensation forcing. Shading intervals are approximately logarithmic.

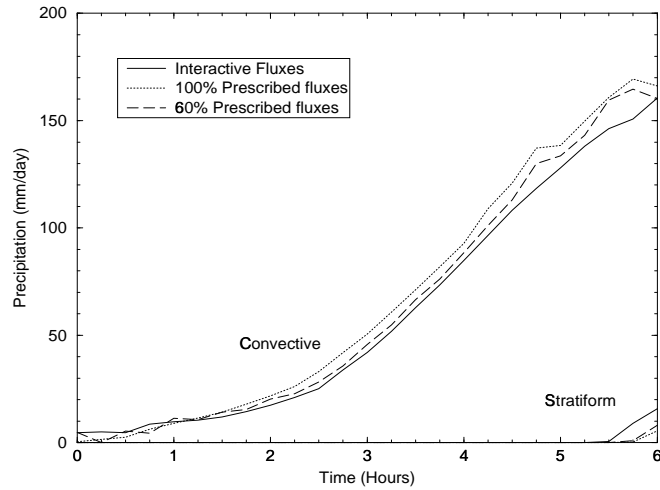


Fig. 7. Case D. Evolution of surface precipitation rate in mm/day, for interactive surface fluxes (solid), 100% prescribed fluxes (dotted) and 60% prescribed fluxes (dashed).

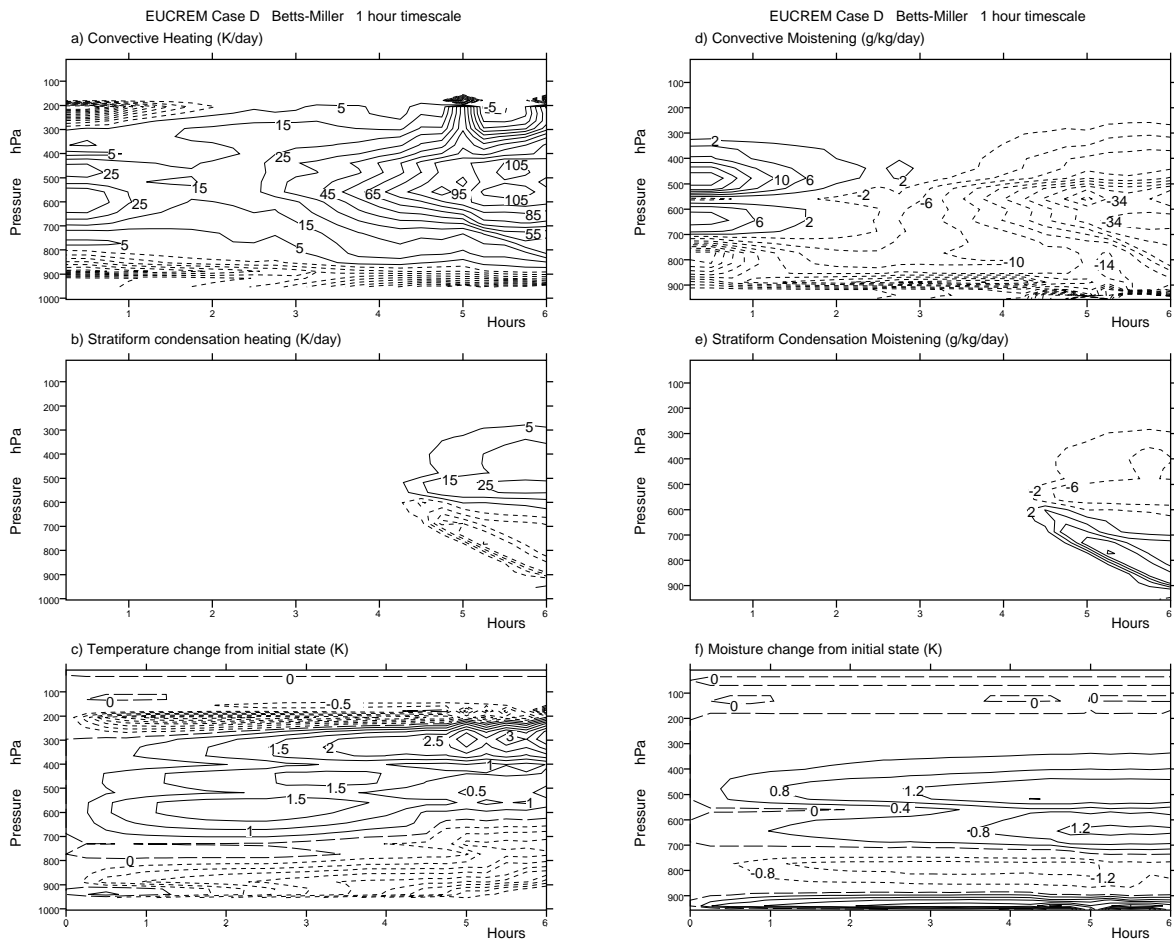


Fig. 8. Case D simulation with a convective adjustment timescale of 1 hour. Heating (left) and moistening (right), due to convection (top) and stratiform condensation (middle). Temperature and moisture evolution as departures from the initial state (bottom).

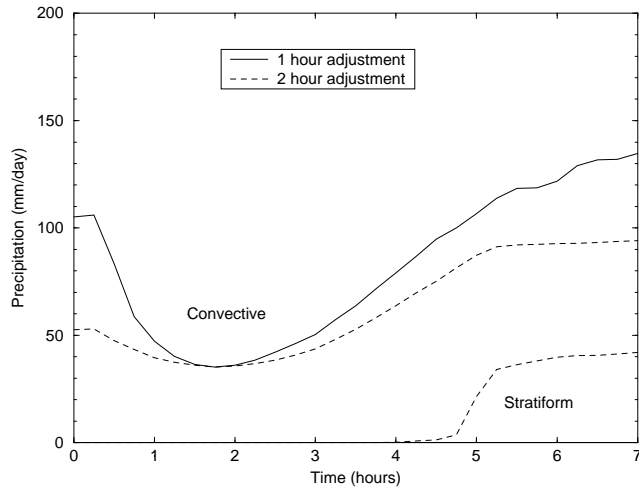


Fig.9. Case E. Evolution of surface precipitation rate in mm/day, for a convective timescale of 1 hour (solid) and 2 hours (dashed).

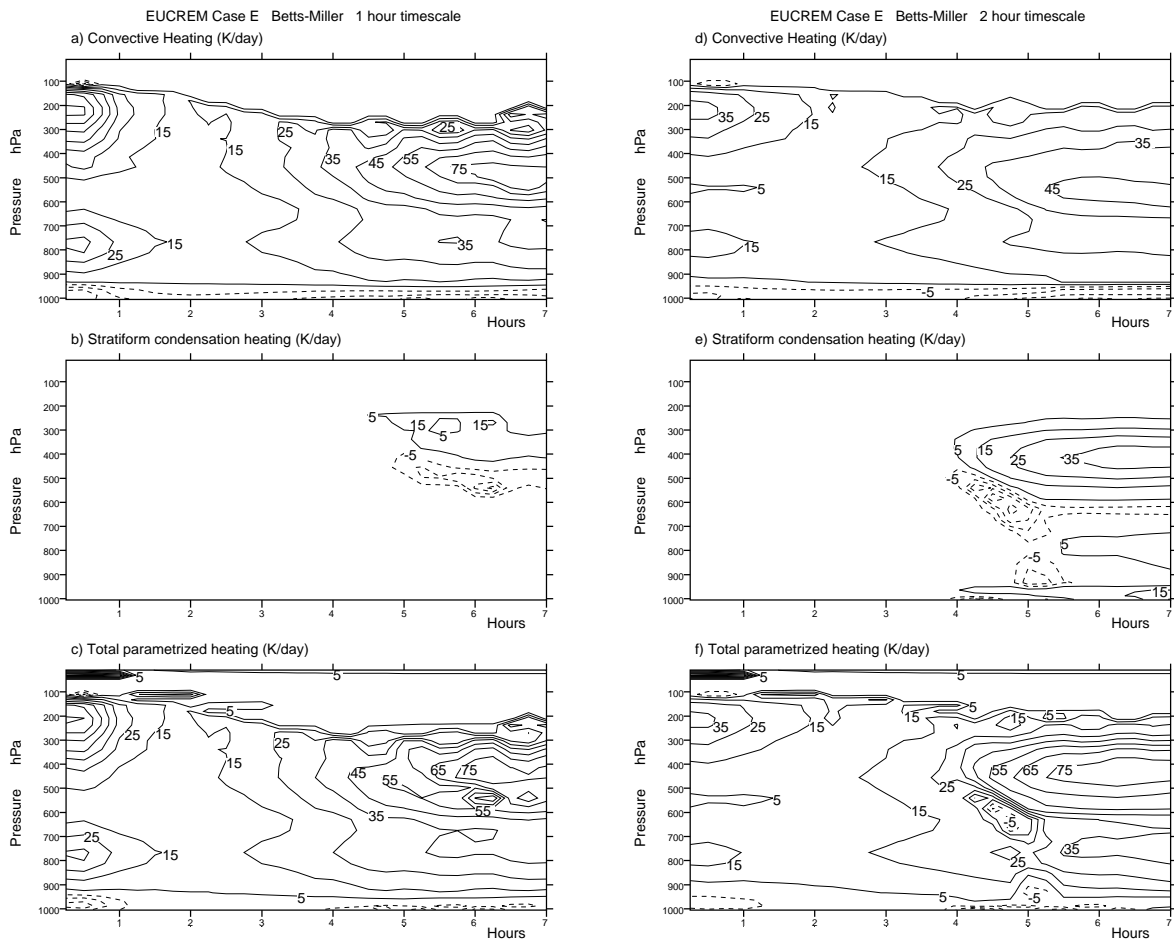


Fig.10. Case E simulations with a convective adjustment timescale of 1 hour (left) and 2 hours (right). Heating rates in K/day for deep convection (top), stratiform condensation (middle) and all parametrizations (bottom).